PAPER REF: 3947 *(Invited Paper)*

BLOOD SIMULATION AND VIRTUAL BYPASS SURGERY

Catarina F. Castro[1,2(*)], Carlos C. António[1,2], Luisa C. Sousa[1,2]

[1]Institute of Mechanical Engineering (IDMEC), University of Porto, Porto, Portugal
[2]Department of Mechanical Engineering (DEMec), University of Porto, Portugal
[(*)]*Email:* ccastro@fe.up.pt

ABSTRACT

Non-invasive medical imaging data acquisition made feasible the definition of high quality surfaces of blood vessels what is crucial to guarantee the correct numerical results on blood flow simulations. In this work, a validated computational blood flow model is used to simulate hemodynamic arterial bypass conditions under physiologic pulsatile conditions. Local hemodynamic parameters near the anastomosis region are found to change substantially with bypass geometry and along the cardiac cycle.

Keywords: modelling, vascular graft, optimization, biomedical technology.

INTRODUCTION

Atherosclerosis is the formation of plaques on the arterial walls, a widespread disease that manifests particularly in developed countries. Treatment often involves surgery, such as the placement of bypasses to lead the blood around clogged arteries restoring normal blood flow.

Researchers have developed artificial graft tissue by combining man-made materials with human cells to make it elastic and durable and so it can be attached to the host artery and efficiently replace the obstructed conduct. Nevertheless, several studies have proven that restenosis phenomena develop in bypass-artery junctions leading to poor performance and failure of the surgery (Giddens, et al., 1993). Initiation and progress of these diseases are not fully understood but thought to be a consequence of physiological response to abnormal conditions of local hemodynamic (Ray, et al., 1997). Hence, patient-specific modeling and accurate numerical simulations provide means to obtain data on hemodynamic parameters (Shaik, 2007; Taylor, et al., 2004).

Computational techniques are becoming an important tool to better understand blood flow characteristics and virtual surgery may be used during pre-operative planning to support surgeon's decisions. Patient-specific modelling of blood flow for bypass graft surgery requires clinical measurements consisting of certain key elements that are essential for a proper diagnosis. Simulation models, both numerical and physical, have been created in hopes to gain better understanding on the relationship between the information contained in the clinical measurements and the complex physical and physiological factors that induces bypass restenosis and failure (Sankaran, et al., 2012; Sottiurai, et al., 1989).

A computational fluid dynamics code can be used to simulate relevant flow fields, where finite element techniques are used to compute flow parameters. Numerical simulations are advantageous over in vitro experiments since they are normally less expensive, can be performed more quickly, and parameters can be more readily changed. However, the assumed velocity fields may be too idealistic. In this work, a virtual bypass surgery is performed by adding an artificial graft to the injured artery. Blood flow behaviour is computed with

predefined geometries using a previously validated finite element code (Sousa, et al., 2012). The resulting flow characteristics are analysed by comparing simulated flow velocities and induced wall shear stresses for different graft systems. Patency rate implications for patient-specific arterial bypass grafts surgery are discussed.

BYPASS SURGERY

An invasive procedure of synthetic vascular grafting is performed when a prosthetic graft is used to create a bridge that bypasses the blocked section of the artery. Intimal hyperplasia is a major cause of stenosis and thrombosis of arterial bypass grafts. The success of synthetic grafts depends on a variety of factors, such as mechanical properties and biocompatibility. With regard to the biocompatibility, the geometry and compliance of the host artery and graft should match. However, achieving such requirements may not be possible in all situations, the diameter of the artery is not equal to the diameter of the graft and/or the mechanical properties of the graft are not similar to the artery. Nevertheless, compliance mismatch alone is not a strong stimulus for intimal hyperplasia. In order to obtain significant intimal hyperplasia, a sutured anastomosis must be present (Ballyk, et al., 1998).

The surgical joining of a vessel with a synthetic graft to allow blood flow from one to the other is known as anastomosis. Fig. 1 presents a schematic representation of the most common anastomoses. For large vessels the end-to-end anastomosis is the simplest, most reliable, and most widely used method. In this type of surgery, the portion of the artery that is blocked is removed, and a graft attached end-to-end. When the portion of the artery that is blocked is not removed, but instead a bypass route is created, the end-to-side is a method used for both smaller and larger vessel surgeries. It has been shown that anastomosis angle effects flow fields and that flow patterns effect graft patency namely, three known locations of bypass graft failure (toe, heel, and arterial floor region) could be minimized by changing the graft anastomosis angles (Trubel, et al., 1995).

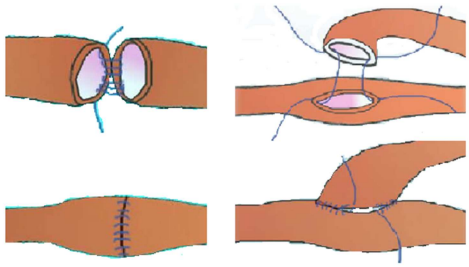

Fig. 1 End-to-end (left) and end-to-side (right) anastomosis (Shaik, 2007)

In end-to-side anastomoses, cellular proliferation occurs preferentially around the suture-line and on the bed of the host artery (Bassiouny, et al., 1992; Sottiurai, et al., 1989). This focal distribution has led investigators to suggest that hemodynamic factors and/or vessel wall mechanical factors may play a role in its pathogenesis. On the bed, it appears that the hyperplasia is induced by adverse fluid shear stress oscillations created by the end-to-side geometry. Around the suture line, however, the tissue thickening is at least partially promoted by graft-artery compliance mismatch (Bassiouny, et al., 1992; Trubel, et al., 2004).

The pattern of suture-induced anastomotic stresses in end-to-end and end-to-side anastomoses indicates that elevated intramural stresses may promote the development of distal anastomotic

suture line intimal hyperplasia. Fig. 2 presents an obstructed artery with a bypass graft (Ballyk, et al., 1998). Dashed lines represent suture lines and intimal hyperplasia is indicated at the heel, toe and bed of the distal junction.

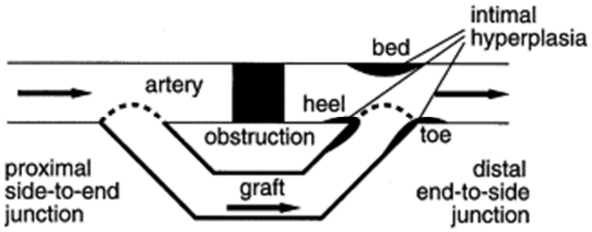

Fig. 2 An obstructed artery with a bypass graft: arrows show systolic blood flow directions (Ballyk, et al., 1998)

In a previous work, steady blood flow simulations through idealized models have shown the influence of anastomosis angles and graft radius on local hemodynamic parameters (Castro, et al., 2010; Castro, et al., 2012). In this work, flow patterns are simulated and wall shear stress calculated assuming a more realistic pulsatile unsteady flow.

BLOOD SIMULATION

In this current study, the numerical analysis of the blood flow phenomena in specific geometric models of bypasses is simulated using the finite element method approach. Fluid is incompressible and governed by the equation of continuity and the Navier-Stokes equations whose viscosity may not be constant. In diseased vessels which are often the subject of interest, the arteries are even less compliant and wall motion is further reduced and the assumption of zero wall motion is used as an approximations. In the present work, biochemical and mechanical interactions between blood and vascular tissue are neglected with boundary conditions similar to physiological circumstances.

The continuity equation is given by

$$\nabla \cdot \mathbf{v} = \mathbf{0} \tag{1}$$

and the momentum balance equation

$$\frac{\partial \mathbf{v}}{\partial \mathrm{t}} + (\nabla \cdot \mathbf{v})\mathbf{v} = -\frac{\mathbf{1}}{\boldsymbol{\rho}} \nabla \mathrm{p} + \boldsymbol{\nu}\, \nabla^2 \mathbf{v} \tag{2}$$

where **v** is the velocity field, $\boldsymbol{\nu}$ the kinematic viscosity, ρ the blood density and p the pressure.

In the numerical simulation, considering the pseudo-constitutive relation for the incompressibility constraint, the continuity equation is replaced by

$$\mathrm{p} = -\frac{\mathbf{1}}{\boldsymbol{\varepsilon}} (\nabla \cdot \mathbf{v}) \tag{3}$$

where 10^8 or 10^9 are generally assigned values to the penalty parameter ε.

The Navier-Stokes equations become:

$$\rho \left(\frac{\partial \mathbf{v}}{\partial \mathrm{t}} + (\nabla \cdot \mathbf{v})\mathbf{v} \right) = \frac{\mathbf{1}}{\boldsymbol{\varepsilon}} \nabla (\nabla \cdot \mathbf{v}) + \mu\, \nabla^2 \mathbf{v} \tag{4}$$

with μ the dynamic viscosity.

Many studies showed that the non-Newtonian property of blood plays an important role in vascular biology and pathology. A non-Newtonian viscosity model is adopted in this project, where viscosity is empirically obtained using Casson law for the shear stress relation

$$\sqrt{\tau} = k_0(c) + k_1(c)\sqrt{\dot{\gamma}} \tag{5}$$

where τ and $\dot{\gamma}$ denote shear stress and shear strain and c the red cell concentration. For generalized 2-D flow, this relation is modified using D_{II} the second invariant of the strain rate tensor. The shear stress τ given by the generalized Casson relation is

$$\sqrt{\tau} = k_0(c) + k_1(c)\sqrt{2\sqrt{D_{II}}} \tag{6}$$

and the apparent viscosity $\mu=\mu(c, D_{II})$ a function of the red cell concentration is,

$$\mu = \frac{1}{2\sqrt{D_{II}}}\tau = \frac{1}{2\sqrt{D_{II}}}\left(k_0(c) + k_1(c)\sqrt{2\sqrt{D_{II}}}\right)^2 \tag{7}$$

where parameters k_0 = 0.6125 and k_1 = 0.174 were obtained fitting experimental data and considering c = 45 percent.

RESULTS

Bypass graft surgeries require surgical construction of a conduit or graft over a blocked blood vessel. For modelling purposes the simplified arterial graft prosthesis is a tubular vessel disposed around a longitudinal axis. A virtual bypass surgery on a 9mm diameter artery is considered. Fig. 3 presents the model including both proximal and distal bypass junctions in order to allow the flow development along the entire bypass. The developed finite element code simulates blood flow in artery and graft using 2261 nodes and 2024 four-node linear elements for a two-dimensional finite element approximation (Sousa, et al., 2012).

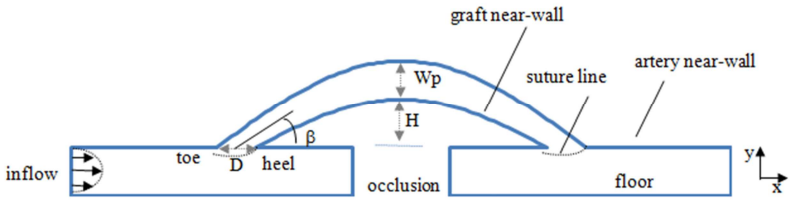

Fig. 3 Anastomotic configuration and nomenclature of the bypass geometry

The considered model depends on a parameter vector **b** of four geometric components **b**=(H,β,Wp,D) as displayed in Fig. 3: the distance from the near wall of the graft to the near wall of the artery H, the junction angle β, the width of the prosthesis at its longitudinal symmetric line Wp and the suture line dimension D.

Blood flow simulations are carried out under physiological pulsatile conditions with velocities varying from zero, when the aortic valve is closed, to high velocities during the systole. Fig. 4 reports the femoral waveform used at in artery inlet, a prescribed inlet velocity waveform (Carneiro, 2009) taken from Taylor and Draney (2004). Inflow conditions at the artery inlet were considered as parabolic velocity profiles. The zero slip velocity boundary condition was employed. For unsteady flow simulations, the code iterates to convergence at each time step and then advances to the following time step performing through a full cardiac cycle. Using

the artery diameter as characteristic length and a reference blood viscosity of μ= 0.035 Poise, the mean reference Reynolds number is given by R_{ref} = 300.

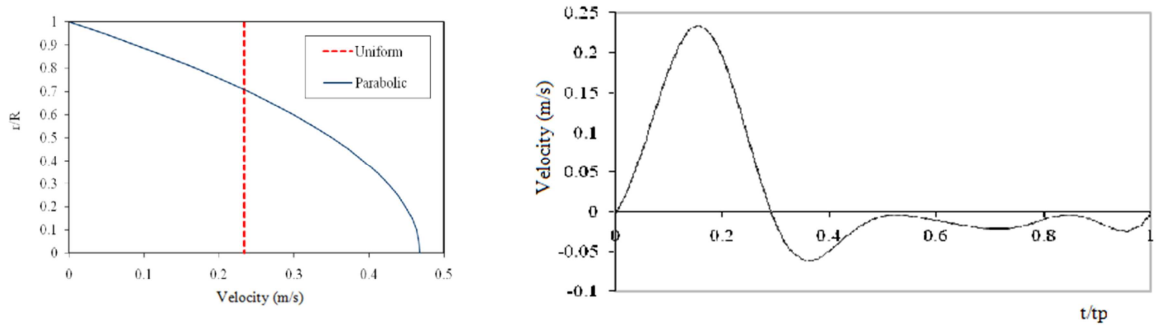

Fig. 4 Inlet velocity profile (left) and waveform (right) described Taylor and Draney (2004) and adapted by Carneiro (2009)

To understand the dependence of blood dynamic behaviour in particular graft geometry, finite element simulations are performed considering four different bypasses calculating hemodynamic parameters, such as velocity and wall shear stress (WSS). Geometry details are reported in Table 1. The prosthetic graft of bypasses A and B is larger than the artery and on the contrary for bypasses C and D the graft is narrower than the artery. The main difference between bypass A and B is the suture line dimension, the suture line of bypass B is the largest. Bypass B presents the smallest junction angle and bypass D presents a smallest distance between artery and graft.

Table 1 Geometric details of the simulated bypasses

Bypass	**H [mm]**	**β [radians]**	**Wp [mm]**	**D [mm]**
A	39.90	0.781	13.89	17.69
B	39.87	0.773	13.84	19.06
C	39.87	0.236	8.050	16.20
D	28.67	0.782	8.114	17.40

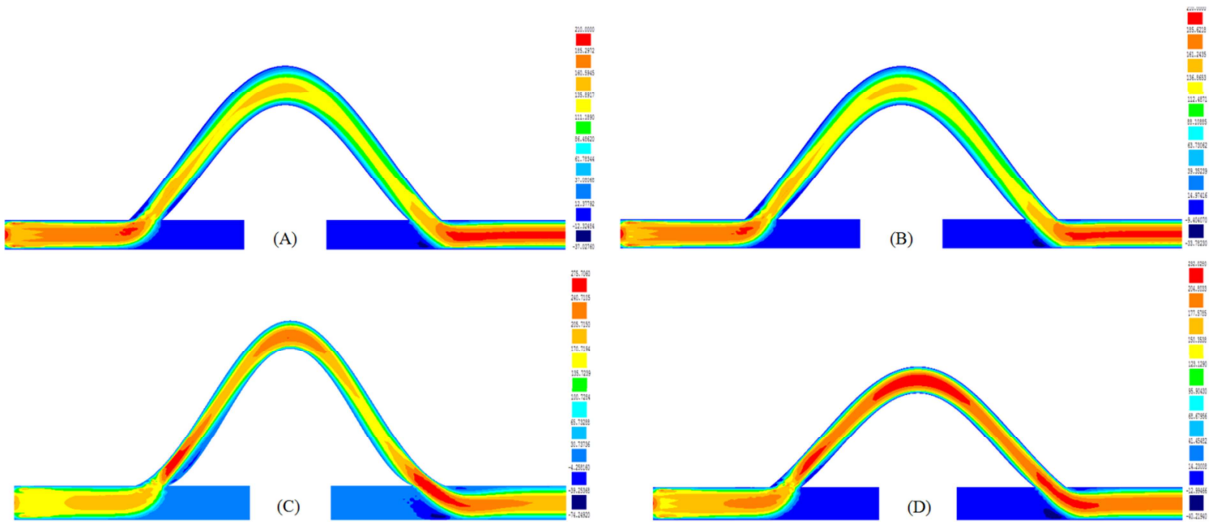

Fig. 5 Longitudinal velocity contours for grafts A, B, C and D (t/tp=0.1)

Results for the simulated longitudinal velocities at the acceleration phase (t/tp=0.1) are showed in Fig. 5. The influence of graft diameter on flow velocity behaviour is obvious. Bypasses A and B present similar flow behaviour with maximal velocities inside the host artery before proximal and after distal junctions. As for bypasses C and D the highest velocity values are attained inside the graft and at the distal junction. A non-symmetric behaviour is obvious for this last bypass D with the fully developed velocity profile being redirected from the native artery into the graft with velocities reaching high values inside the prosthesis just after the proximal anastomosis. Velocity disturbances are mostly evident in the vicinity of the proximal and distal artery-graft junctions. In these regions, simulations show recirculation and low-velocity zones suggesting that both, proximal and distal, regions are responsible for early bypass graft failure.

As blood flows through the lumen, WSS is generated to retard the flow, representing the force acting tangentially to the surface due to friction. For non-slip wall conditions, the properties of the flow adjacent to the wall/fluid boundary are used to predict the shear stress on the fluid at the wall. Since the blood flow is highly skewed, the distributions of the WSS must be measured by detailed velocity profiles very close to the wall.

At the acceleration phase (t/tp=0.1) the distributions of WSS along the distal artery floor are illustrated in Fig. 6 together with the velocity behaviour at the distal junction cross-section. For the four bypass models, results show low WSS values just before the abrupt graft and artery connection and large WSS values induced by the large velocity variations assigned to the same region. Using regions of low wall shear stresses as a measure of undesirable (stagnant) flow patterns, it has been observed that these regions are correlated with three known locations of graft failure (toe, heel, and arterial floor region) and that they could be minimized by changing the graft anastomosis angles and other parameters. Bypass C is designed by using a small junction angle, a small prosthetic graft diameter and a small suture line. Then extreme positive and negative velocity simulated values are plotted in Fig. 6. The profile is asymmetric and skewed towards the upper artery wall.

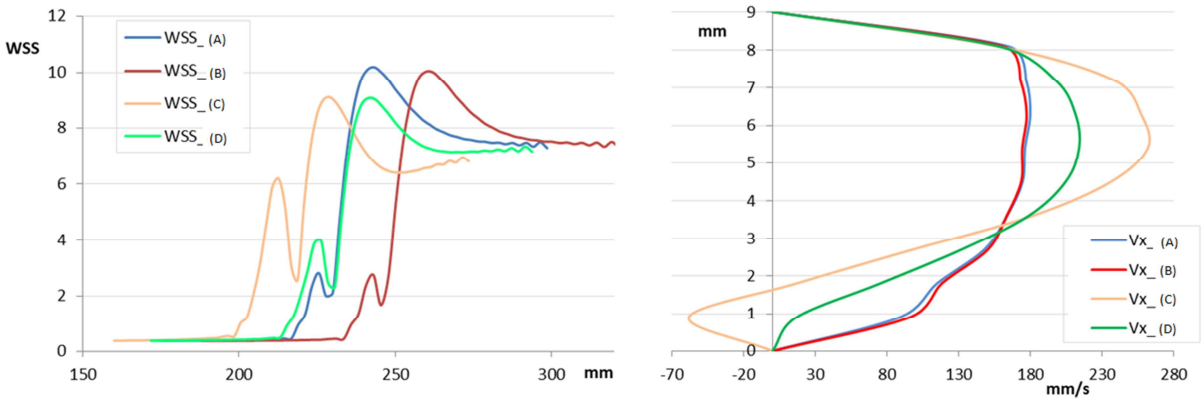

Fig. 6 Comparison of the WSS (left) and velocity (right) for bypasses A, B, C and D (t/tp=0.1)

The velocity variability of bypass C demonstrates the good quality of the finite element code being capable of capturing the flow acceleration as it emerges from the graft to the artery and the flow recirculation at the floor of the host artery, consistently with the expectations. Long residence times, usually observable immediately after the toe of the distal anastomosis, are associated to poor bypass patency.

For bypass D, Fig. 7 reports velocity profiles for different times illustrating the different phases of the cardiac cycle: acceleration phase (t/tp=0.07), peak systole (t/tp=0.16) and deceleration phase (t/tp=0.24 and t/tp=0.26 and t/tp=0.36). Results of the unsteady solution are compared with a simple non-transient solution. For the femoral velocity waveform peri-anastomotic blood velocity distributions are very complex and dominated by unsteadiness. Comparing the velocity profiles along the cardiac cycle it can be concluded that flow patterns are very different. The prime region of disturbed flow patterns is detected by the recirculation zone at the artery floor of distal junction during systolic peak. A region of slow-moving fluid along the lower wall of the host artery, resulting in a stagnation point on the host artery bed is produced. The rapid deceleration phase of the femoral waveform, causes extensive retrograde flow during the late deceleration portion of the flow waveform (t/tp=0.36).This pattern would have been undetected if a non-transient analysis had been used instead.

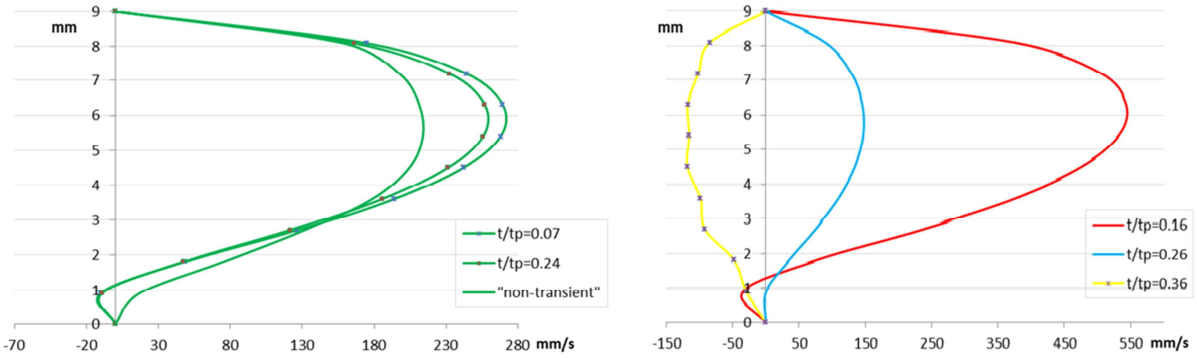

Fig. 7 Velocity behaviour along the cardiac cycle at the distal graft artery junction for bypass D

CONCLUSIONS

This study demonstrates the relevance of numerical simulation models applied to arterial bypass surgery. Blood flow behavior is shown to be sensitive to the bypass geometry and to have a strong influence on local quantities of interest that would potentially affect bypass longevity. A detailed understanding of flow will aid in the evaluation of therapeutic options available to a given patient and especially before vascular surgery or artificial grafts are implanted. Typically, there are many solutions for a bypass surgery. Thus, it is often necessary to incorporate surgeon preferences in order to determine a suitable solution. Future work plans to analyze patient-specific bypass surgeries. Further validation with post-surgical clinical data is needed.

The study reported herein establishes the methodology as a viable means of achieving virtual bypass surgeries. The importance of designing optimized bypass graft cannot be neglected.

ACKNOWLEDGMENTS

The authors thank the financial support of FCT – Fundação para a Ciência e a Tecnologia from Portugal, through Unidade de Investigação: 10/225 - Unit for Numerical Methods in Mechanics and Structural Engineering, IDMEC – Pólo FEUP and project PTDC/SAU-BEB/102547/2008, Blood flow simulation in arterial networks towards application at hospital.

REFERENCES

Ballyk PD, Walsh C, Butany J, Ojha M. Compliance mismatch may promote graft-artery intimal hyperplasia by altering suture-line stresses. Journal of Biomechanics, 1998, 31, p.229-237.

Bassiouny HS, White S, Glagov S, Choi E, Giddens DP, Zarins C K. Anastomotic intimal hyperplasia: mechanical injury or flow induced. J. Vas. Surg., 1992, 15, 708-716.

Carneiro AF. Influência do ciclo cardíaco no fluxo sanguíneo na vizinhança da bifurcação ilíaca. (2009) Escola de Engeharia da Universidade do Minho, Portugal: PhD Thesis.

Castro CF, António CC, Sousa LC. Multi-objective optimization of bypass grafts in arteries. TMSi - Sixth International Conference on Technology and Medical Sciences, Porto, Portugal, 2010, p. 191-196.

Castro CF, António CC, Sousa LC. Optimização da geometria de próteses arteriais: caso estacionário. Revista Iberoamerica de Engeniería Mecánica, 2012, 16(2), p.19-27.

Giddens DP, Zarins CK, Glagov S. The role of fluid mechanics in the localization and detection of atherosclerosis. J. Biomech. Eng., 1993, 115, p.588-594.

Ray SA, Rowley MR, Bevan DH, Taylor RS, Dormandy JA. Hypercoagulable abnormalities and postoperative failure of arterial reconstruction. Eur Journal Vasc Endovasc Surg., 1997, 13(4), p.363-370.

Sankaran S, Moghadam ME, Kahn AM, Tseng EE, Guccione J L, Mardsen AL. Patient-Specific Multiscale Modeling of Blood Flow for Coronary Artery Bypass Graft Surgery. Annals of Biomedical Engineering, 2012, 40(10), p.2228-2242.

Shaik E. Numerical Simulations of Blood flow in arteries using Fluid-Structure Interactions. (2007) Wichita State University, PhD.

Sottiurai VS, Yao JS, Batson RC, Sue SL, Jones R, Nakamura, YA. Distal anastomotic intimal hyperplasia: histopathological character and biogenesis. Annals of Vascular Surgery, 1989, 1, p.26–33.

Sousa LC, Castro CF, António CC, Chaves R. Blood flow simulation and vascular reconstruction. Journal of Biomechanics, 2012, 45, p.2549-2555.

Sousa L, Castro CF, Antonio CA, Chaves R. Computational Techniques and Validation of Blood Flow Simulation. WEAS Transactions on Biology and Biomedicine, Included in ISI/SCI Web of Science and Web of Knowledge, 2011, 4-8, p.145-155.

Taylor CA, Draney M. Experimental and Computational Methods in Cardiovascular and Fluid Mechanics. Annual Review of Fluid Mechanics, 2004, 36, p.197-231.

Trubel W, Schima H, Czerny M, Perktold K, Schimek MG, Poltrerauer P. Experimental comparison of four methods of end-to-side anastomosis with expanded polytetra-fluoroethylene. British J. Surg., 2004, 91, p.159-167.

Trubel W, Schima H, Moritz A, Raderer F, Windisch A, Ullrich R, Polterauer P. Compliance mismatch and formation of distal anastomotic intimal hyperplasia in externally stiffened and lumen-adapted venous grafts. Eur J Vasc Endovac Surg, 1995, 10, p.415-423.